Mutation Research - Genetic Toxicology and Environmental Mutagenesis 891 (2023) 503694

Contents lists available at ScienceDirect

Mutation Research - Genetic Toxicology and Environmental Mutagenesis

journal homepage: www.elsevier.com/locate/gentox

Myricetin causes site-specific DNA damage via reactive oxygen species generation by redox interactions with copper ions

Yuichiro Hirao [a,b], Hatasu Kobayashi [a], Yurie Mori [a], Shinya Kato [c], Shosuke Kawanishi [d], Mariko Murata [a], Shinji Oikawa [a,*]

[a] Department of Environmental and Molecular Medicine, Mie University Graduate School of Medicine, Tsu, Mie, Japan
[b] Department of Home Care Nursing, Mie Prefectural College of Nursing, Tsu, Mie, Japan
[c] Radioisotope Experimental Facility, Advanced Science Research Promotion Center, Mie University, Tsu, Mie, Japan
[d] Faculty of Pharmaceutical Sciences, Suzuka University of Medical Science, Suzuka, Mie, Japan

ARTICLE INFO

Keywords:
8-oxo-7,8-dihydro-2′-deoxyguanosine
Mutagen
Pro-oxidant
Phenolic compound
Pharmacological activity

ABSTRACT

Myricetin (MYR), found in tea and berries, may have preventive effects on diseases, including Alzheimer's disease and cancer. However, MYR is also a mutagen, inducing DNA damage in the presence of metal ions. We have studied the molecular mechanisms of DNA damage by MYR in the presence of Cu(II) (MYR+Cu). Using ^{32}P-5′-end-labeled DNA fragments, we analyzed site-specific DNA damage caused by MYR+Cu. MYR+Cu caused concentration-dependent DNA strand breaks and base alterations, leading to cleavage of DNA at thymine, cytosine, and guanine nucleotides. Formation of the oxidative DNA damage indicator, 8-oxo-7,8-dihydro-2′-deoxyguanosine (8-oxodG), in calf thymus DNA was increased by MYR+Cu. The production of 8-oxodG in MYR-treated HL-60 cells was significantly higher than in HP100 cells, which are more resistant to H_2O_2 than are HL-60 cells. Reactive oxygen species (ROS) scavengers were used to elucidate the mechanism of DNA damage. DNA damage was not inhibited by typical free hydroxyl radical (•OH) scavengers such as ethanol, mannitol, or sodium formate. However, methional, catalase, and bathocuproine inhibited DNA damage induced by MYR+Cu. These results suggest that H_2O_2, Cu(I), and ROS other than •OH are involved in MYR+Cu-induced DNA damage. We conclude that the Cu(I)/Cu(II) redox cycle and concomitant H_2O_2 production via autoxidation of MYR generate a complex of H_2O_2 and Cu(I), probably Cu(I)-hydroperoxide, which induces oxidative DNA damage.

1. Introduction

Myricetin (3,5,7-trihydroxy-2-(3,4,5-trihydroxyphenyl)-4-chromenone, MYR) is a phenolic compound found in many plants, including tea, berries, vegetables, grapes, and walnuts [1]. Recently, it has been suggested that MYR may protect against Alzheimer's disease (AD) and cancer. AD is the most common form of dementia, accounting for 60–70 % of cases. Accumulating amyloid-β (Aβ) peptide in the brain is hypothesized to be the initial pathological event in AD progression [2]. Ono et al. found that MYR inhibited Aβ peptide oligomerization [3]. MYR prevented the development of AD pathology in mouse models [4]. In addition, MYR is cytotoxic to many human cancer cell lines. MYR induces apoptosis of HCT-15 human colon cancer cells [5]. MYR also protects against skin cancer by strongly inhibiting neoplastic cell transformation [6]. In a cohort study, Geybels et al. reported that higher intake of MYR lowered the risk of advanced prostate cancer [7]. Based on these findings, MYR is a possible prophylactic agent for AD and cancer.

In contrast, MYR is positive in bacterial mutagenicity and in vitro micronucleus formation assays [8]. MYR, in the presence of metal ions, induces DNA damage via reactive oxygen species (ROS) generation [9–12]. However, the molecular mechanism of MYR-induced DNA damage has not been fully elucidated. Here, we investigated the molecular mechanism of DNA damage induced by MYR in the presence of Cu(II) (MYR+Cu). Using ^{32}P-5′-end-labeled DNA fragments, we analyzed DNA damage and its site specificity on DNA base sequences. Using high-performance liquid chromatography (HPLC) equipped with an electrochemical detector (HPLC-ECD), we measured the amount of 8-oxo-7,8-dihydro-2′-deoxyguanosine (8-oxodG), an indicator of oxidative DNA damage, formed in calf thymus DNA treated with MYR. We

* Correspondence to: Department of Environmental and Molecular Medicine, Mie University Graduate School of Medicine, Edobashi 2-174, Tsu, Mie 514-8507, Japan.
E-mail address: s-oikawa@med.mie-u.ac.jp (S. Oikawa).

https://doi.org/10.1016/j.mrgentox.2023.503694
Received 24 May 2023; Received in revised form 14 September 2023; Accepted 16 September 2023
Available online 18 September 2023

also used the HL-60 human leukemia cell line and its H_2O_2-resistant clone HP100 to examine intracellular 8-oxodG production.

2. Materials and methods

2.1. Materials

T_4 polynucleotide kinase, *Eco*RI, APE1 (10,000 units/ml, human, recombinant), and endonuclease IV (10,000 units/ml, *Escherichia coli*, recombinant) were purchased from New England Biolabs Ltd. (Ipswich, MA). *Bss*HII and *Pst*I were purchased from Takara Bio Inc. (Shiga, Japan). [γ-^{32}P] ATP (222 TBq/mmol) was purchased from Perkin Elmer, Inc. (Waltham, MA, USA). Bacterial alkaline phosphatase (from *Escherichia coli*), 3-(methylthio) propionaldehyde (methional), catalase (30,000 units/mg from bovine liver), and superoxide dismutase (SOD) (3000 units/mg from bovine erythrocytes, Cu/Zn) were purchased from Sigma-Aldrich (St Louis, MO). MYR was purchased from Tokyo Chemical Industry Co., Ltd. (Tokyo, Japan). Copper(II) chloride dihydrate ($CuCl_2 \cdot 2H_2O$), ethanol (EtOH), mannitol, and sodium formate were purchased from Nacalai Tesque (Kyoto, Japan). Nuclease P_1 (500 units/vial) and piperidine were purchased from FUJIFILM Wako Pure Chemical Co., Ltd. (Osaka, Japan). Calf intestinal phosphatase (500 units/vial) was purchased from Roche Diagnostics GmbH (Mannheim, Germany). Diethylenetriamine-*N,N,N′,N″,N″*-pentaacetic acid (DTPA) and bathocuproine disulfonic acid were purchased from Dojindo Laboratories (Kumamoto, Japan).

2.2. Preparation of ^{32}P-5′-end-labeled DNA fragments

The human *p16* tumor suppressor gene [13] and the c-Ha-*ras*-1 protooncogene [14] were used as DNA fragments. The DNA was dephosphorylated with calf intestinal phosphatase and phosphorylated with [γ-^{32}P] ATP and T4 polynucleotide kinase. The DNA fragment containing exon 2 of the human *p16* tumor suppressor gene was obtained as described previously [15]. The ^{32}P-5′-end-labeled 460 base pair (bp) fragment (*Eco*RI* 9481-*Eco*RI* 9940) containing exon 2 was further digested with *Bss*HII to obtain the singly labeled 309 bp fragment (*Eco*RI* 9481–*Bss*HII 9789) and the 147 bp fragment (*Bss*HII 9794–*Eco*RI* 9940). The c-Ha-*ras*-1 fragment was prepared from plasmid pbcNI, which carries a 6.6-kb *Bam*HI chromosomal DNA restriction fragment [16]. The ^{32}P-5′-end-labeled 435 bp fragment was digested with *Pst*I to obtain the singly labeled 337 bp fragment (*Pst*I 2345-*Ava*I* 2681) and the 98 bp fragment (*Ava*I* 2247–*Pst*I 2344). The asterisk indicates ^{32}P-labeling.

2.3. Analysis of DNA damage caused by MYR+Cu

MYR was added to reaction mixtures in 1.5 ml Eppendorf microtubes containing ^{32}P-5′-end-labeled DNA fragments, 20 μM/base calf thymus DNA and 20 μM $CuCl_2$ in 10 mM sodium phosphate buffer (pH 7.8), 200 μl, containing 5 μM DTPA. Denatured single-stranded DNA fragments were prepared by heating at 90 °C for 5 min followed by rapid cooling before the addition of MYR. ROS scavengers and bathocuproine were added before the addition of MYR. The reaction mixtures were incubated at 37 °C for 1 h under light shielding. After incubation, the DNA fragments were heated in 10 % piperidine at 90 °C for 20 min. The DNA fragments were electrophoresed on an 8 % polyacrylamide/8 M urea gel. An autoradiogram was obtained by exposing an X-ray film (FUJIFILM Corp., Tokyo, Japan) to the gel as described previously [17,18].

Preferred cleavage sites were determined by directly comparing the positions of the oligonucleotides with those produced by the chemical reactions of the Maxam–Gilbert method [19] using a DNA-sequencing system (LKB 2010 Macrophor, LKB Pharmacia Biotechnology Inc., Uppsala, Sweden). The autoradiogram was obtained by exposing an imaging plate (BAS-MS2040, FUJIFILM Corp.) to the gel. The relative amounts of oligonucleotides from the treated DNA fragments were measured using a laser scanner (Typhoon FLA-9500, GE Healthcare, Buckinghamshire, England) and analyzed with Image Quant TL software (GE Healthcare).

2.4. Analysis of 8-oxodG formation in calf thymus DNA by MYR+Cu

Measurement of 8-oxodG was performed as described previously [20]. The reaction mixtures, containing 100 μM/base calf thymus DNA, MYR and 20 μM $CuCl_2$ in 4 mM sodium phosphate buffer (pH 7.8), 400 μl, containing 5 μM DTPA, were incubated at 37 °C for 1 h under light shielding. After EtOH precipitation, the DNA fragments were digested to nucleosides with nuclease P_1 and calf intestinal phosphatase. The amount of 8-oxodG was measured by HPLC-ECD as described previously [21,22]. To clarify the role of O_2 in 8-oxodG formation through autoxidation, the reaction mixtures containing MYR +Cu were made hypoxic by bubbling with N_2 gas for 1 min

2.5. Analysis of 8-oxodG formation in cultured cells treated with MYR

Human leukemia HL-60 and its H_2O_2-resistant clone HP100 cells were grown in RPMI 1640 medium supplemented with 10 % fetal bovine serum at 37 °C under 5 % CO_2. HL-60 and HP100 cells were harvested by centrifugation. Cells (10^7 cells) were incubated with MYR at 37 °C for 16 h and immediately washed twice with PBS. DNA was extracted using a DNA Extractor WB Kit (FUJIFILM Wako Pure Chemical Industries, Ltd). To avoid artificial formation of 8-oxodG, deferoxamine mesylate, which chelates traces of redox-active iron, was added to the lysis solution included in the kit for cellular DNA extraction, in accordance with a previous report [23]. The DNA was dissolved in H_2O and treated with nuclease P_1, 8 U, followed by bacterial alkaline phosphatase, 1.2 U. 8-OxodG content was determined by a previously described method [24,25].

3. Results

3.1. Damage of ^{32}P-5′-labeled DNA fragments by MYR+Cu

An autoradiogram of DNA fragments incubated with various concentrations of MYR+Cu and followed by treatment with or without piperidine is shown (Fig. 1). Oligonucleotides were detected on the autoradiogram as a result of DNA damage. MYR+Cu caused DNA damage (Fig. 1). DNA damage increased with MYR concentration and was further enhanced by piperidine treatment (Fig. 1). The base

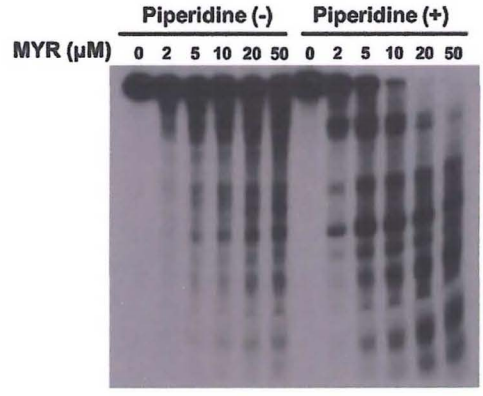

Fig. 1. Autoradiogram of ^{32}P-5′-end-labeled DNA fragments incubated with MYR+Cu. Reaction mixtures contained the ^{32}P-5′-end-labeled 309 bp fragment, 20 μM/base calf thymus DNA, the indicated concentrations of MYR and 20 μM $CuCl_2$ in 10 mM sodium phosphate buffer (pH 7.8) containing 5 μM DTPA. After incubation at 37 °C for 1 h under light shielding, the DNA fragments were treated with or without piperidine and electrophoresed on a polyacrylamide gel.

modification was likely induced by MYR+Cu because the altered base is readily removed from its sugar by piperidine treatment. To confirm apurinic-apyrimidinic (AP) site formation, we performed experiments using AP endonucleases instead of piperidine and showed AP site formation by MYR+Cu (data not shown). These results suggested that MYR+Cu causes base lesions such as base modification and AP site formation, in addition to breaking the sugar-phosphate backbone of DNA. MYR+Cu-induced DNA damage in single-stranded DNA was greater than in double-stranded DNA (Fig. S1).

3.2. Site specificity of DNA damage induced by MYR+Cu

The site specificity of DNA damage induced by MYR+Cu is shown in Fig. 2. MYR+Cu cleaved DNA at thymine and cytosine nucleotides in DNA fragments obtained from the *p16* tumor suppressor gene with piperidine treatment (Fig. 2A and B). In DNA fragments obtained from the human c-Ha-*ras*-1 protooncogene, MYR+Cu caused piperidine-labile lesions at guanine in addition to thymine and cytosine residues (Fig. 2C and D).

3.3. Formation of 8-oxodG in calf thymus DNA by MYR+Cu

Formation of 8-oxodG in calf thymus DNA treated with MYR+Cu is shown (Fig. 3). 8-OxodG is considered to be a product generated when ROS reacts with DNA. The content of 8-oxodG in calf thymus DNA increased in a MYR-concentration-dependent manner. MYR+Cu yielded lower amounts of 8-oxodG under hypoxic conditions than under normoxic conditions.

3.4. Formation of 8-oxodG in human cultured cells by MYR

We examined the intracellular production of 8-oxodG in HL-60 and HP100 cells. Compared with HL-60 cells, HP100 cells are approximately

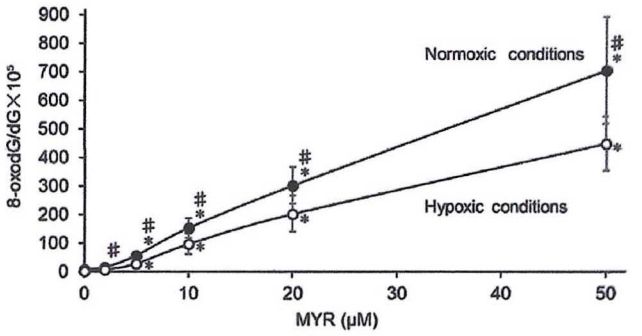

Fig. 3. Formation of 8-oxodG in calf thymus DNA induced by MYR+Cu. Reaction mixtures contained 100 μM/base calf thymus DNA, the indicated concentrations of MYR and 20 μM $CuCl_2$ in 4 mM sodium phosphate buffer (pH 7.8) containing 5 μM DTPA. Reaction mixtures were incubated at 37 °C for 1 h under light shielding. After EtOH precipitation, the DNA was digested to nucleosides with nuclease P_1 and calf intestinal phosphatase and then analyzed by HPLC-ECD. Results are expressed as means ± SD obtained from five independent experiments. Significance was analyzed using the *t*-test. $^{*}p < 0.05$ vs. 0 μM. $^{\#}p < 0.05$ vs. hypoxic conditions.

340-fold more resistant to H_2O_2 [26]. An increase in intracellular 8-oxodG levels was observed when HL-60 cells were treated with MYR (Fig. 4). 8-OxodG formation in HL-60 cells increased in a MYR-concentration-dependent manner at 0.1–0.2 mM and plateaued at 0.5 mM. The levels of 8-oxodG in HL-60 cells treated with 0.1, 0.2, or 0.5 mM MYR were higher than in HP100 cells. These results suggested that H_2O_2 is involved in MYR-induced 8-oxodG formation.

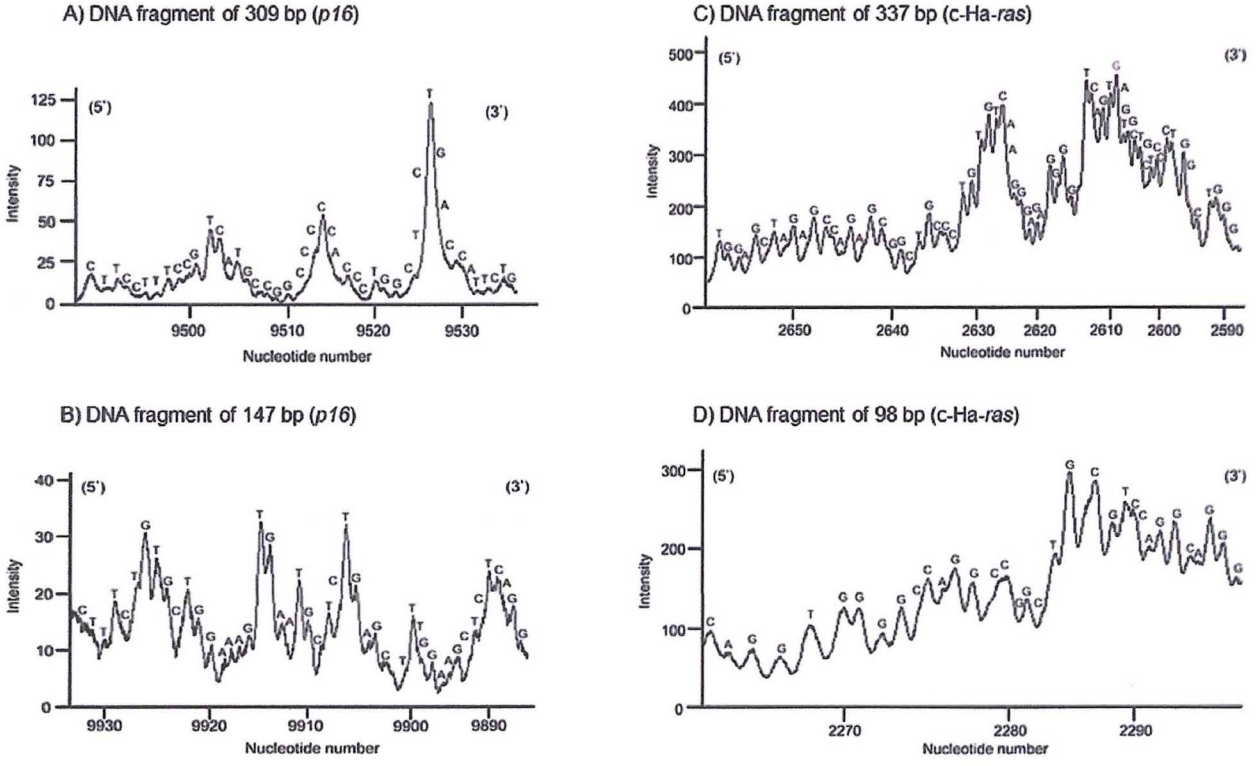

Fig. 2. Site specificity of MYR+Cu-induced DNA damage. Reaction mixtures contained the ^{32}P-5'-end-labeled 309 bp, 147 bp, 337 bp or 98 bp fragment, 20 μM/base calf thymus DNA, 30 μM MYR and 20 μM $CuCl_2$ in 10 mM sodium phosphate buffer (pH 7.8) containing 5 μM DTPA. After incubation at 37 °C for 1 h under light shielding, the DNA fragments were treated with piperidine and electrophoresed on a polyacrylamide gel.

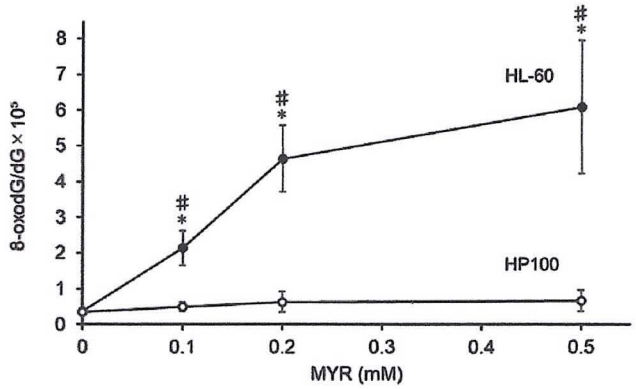

Fig. 4. Formation of 8-oxodG in human cultured cells treated with MYR. HL-60 and HP100 cells (10^7 cells) were incubated with the indicated concentrations of MYR in RPMI-1640 medium supplemented with 10 % fetal bovine serum for 16 h. After incubation, DNA was extracted immediately, subjected to enzymatic digestion and analyzed by HPLC-ECD, as described in Materials and methods. Results are expressed as means ± SD from three to six independent experiments. Significance was analyzed using the *t*-test. $^{*}p < 0.05$ vs. 0 mM. $^{\#}p < 0.05$ vs. HP100.

3.5. *Effects of scavengers and bathocuproine on DNA damage induced by MYR+Cu*

We examined the effects of various scavengers and bathocuproine on the damage of ^{32}P-5′-labeled DNA fragments by MYR+Cu (Fig. 5). DNA damage was not inhibited by typical free hydroxyl radical (•OH) scavengers such as EtOH, mannitol, or sodium formate. In contrast, DNA damage was inhibited by methional, a scavenger of various ROS [27]. Catalase, which decomposes H_2O_2 [28] and bathocuproine, a Cu (I)-specific chelator [29], also inhibited DNA damage. DNA damage was not inhibited by adding SOD, which catalyzes the dismutation of the superoxide anion radical ($O_2^{\bullet-}$) into O_2 and H_2O_2.

4. Discussion

In this study, we showed concentration-dependent DNA damage induced by MYR+Cu, using ^{32}P-5′-labeled DNA fragments. Piperidine and AP endonuclease treatment indicated that MYR+Cu causes base modification and AP site formation in addition to breaking the sugar-phosphate backbone. We analyzed the site specificity of DNA damage with piperidine treatment, using the Maxam–Gilbert sequencing method. MYR+Cu cleaved DNA at thymine, cytosine, and guanine nucleotides in the *p16* tumor suppressor gene and human c-Ha-*ras*-1 protooncogene. DNA cleavage at nucleotides other than adenine is similar to the results of our previous studies investigating DNA damage by ROS-generating agents plus Cu(II) [30,31]. Oxidatively modified adenines have been reported to be less abundant than other nucleotides and, in addition, are resistant to piperidine treatment [32]. These previous observations may explain why little cleavage of DNA at adenine was observed.

We measured the formation of 8-oxodG, an indicator of the oxidative DNA products [33], to assess whether MYR+Cu induces oxidative DNA damage. MYR+Cu significantly increased the formation of 8-oxodG in calf thymus DNA. When dissolved O_2 in the reaction mixtures containing MYR+Cu was removed by bubbling N_2 gas, formation of 8-oxodG was reduced. These results suggest the involvement of O_2 in MYR+Cu-induced DNA damage. Analysis of 8-oxodG in MYR-treated cultured cells showed that more 8-oxodG was produced in HL-60 cells than in HP100 cells. Catalase activity is higher in HP 100 cells than in HL-60 cells [26]. Our previous report demonstrated that treatment with a catalase inhibitor, 3-aminotriazole, significantly increases 8-oxodG formation by homocysteine in HP100 cells compared to HP100 cells without

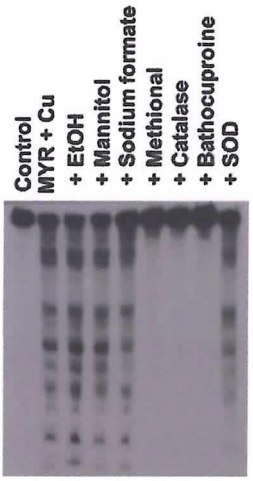

Fig. 5. Effects of scavengers and bathocuproine on MYR+Cu-induced DNA damage. Reaction mixtures contained the ^{32}P-5′-end-labeled 309 bp fragment, 20 μM/base calf thymus DNA, 20 μM MYR, each scavenger or bathocuproine and 20 μM $CuCl_2$ in 10 mM sodium phosphate buffer (pH 7.8) containing 5 μM DTPA. After incubation at 37 °C for 1 h under light shielding, the DNA fragments were treated with piperidine and electrophoresed on a polyacrylamide gel. The concentration of each scavenger and bathocuproine were as follows: 0.8 M EtOH, 0.1 M mannitol, 0.1 M sodium formate, 0.1 M methional, 30 U catalase, 50 μM bathocuproine and 30 U SOD.

3-aminotriazole treatment [34]. Thus, the generation of H_2O_2 may play an important role in forming 8-oxodG by MYR. 8-OxodG is a premutagenic lesion in mammalian cells. Numerous studies have indicated that the formation of 8-oxodG causes misreplication of DNA that may lead to mutations such as G→T transversions in tumor-relevant genes [35,36].

The mechanism of DNA damage was clarified by examining the effects of various scavengers. MYR+Cu-induced DNA damage was inhibited by methional, catalase, or bathocuproine but not by the typical •OH scavengers, EtOH, mannitol, or sodium formate. SOD did not inhibit DNA damage. These results suggest that H_2O_2, Cu(I) and ROS other than •OH are involved in DNA damage by MYR+Cu. Based on these results, we propose a mechanism of oxidative DNA damage induced by MYR+Cu (Fig. 6). The redox cycle of Cu(I)/Cu(II) and concomitant H_2O_2 production, possibly via autoxidation of MYR, generates a complex of H_2O_2 and Cu(I), probably Cu(I)-hydroperoxide, which induces oxidative DNA damage. Copper is thought to play a central role in DNA damage induced by MYR. Copper ions are particularly adept at enhancing mutagenic activities caused by increased ROS [37,38]. In addition, cancer cells, including colon and prostate cancer cells, have been reported to contain high levels of copper, postulated to be important for the carcinogenic process [39,40].

We previously reported the mechanism of DNA damage by quercetin [41], which has a structure similar to MYR. In the present study, we compared DNA damage by kaempferol, quercetin, and MYR under the same conditions (Fig. S2). MYR induced extensive DNA damage in the presence of Cu(II) when compared with quercetin. In contrast, kaempferol induced minimal or no DNA damage. MYR caused DNA damage in a dose-dependent manner, whereas 50 μM quercetin caused the greatest amount of DNA damage. What causes this observed difference in DNA damage by these compounds? The spin density map of the kaempferol radical (K•) shows that its unpaired electron (UE) is concentrated on C2 and C3, and partly on its B ring. In the quercetin radical (Q•), the UE is less concentrated on the C2 and C3 positions and resides more in the B ring compared with the UE of K• [42]. The difference between the MYR radical (M•) and K• (i.e., less on the C2 and C3 and more in ring B) is even more pronounced than the difference between Q• and K•. These observations indicate that the negatively charged O in ring B greatly

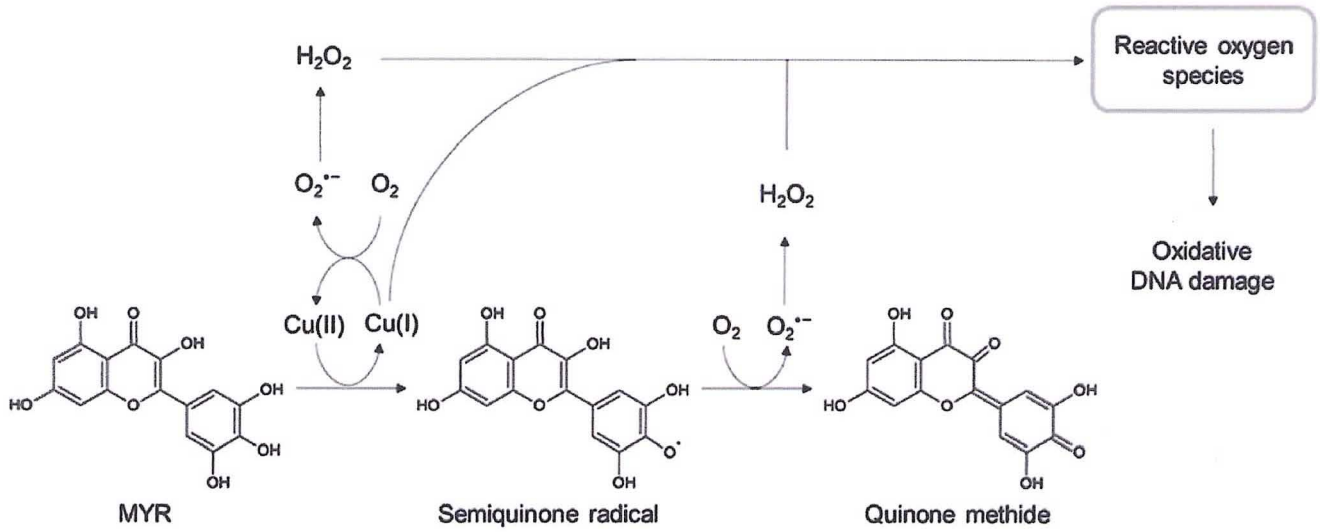

Fig. 6. A possible mechanism of oxidative DNA damage induced by MYR+Cu.

attracts and stabilizes the UE. Thus, our result may be explained by differences in the enrichment of the UE going from K• to Q• to M•, which respectively contain one, two and three deprotonated hydroxyl groups in the B ring. Consequently, Q• and M• are more likely to donate a second electron than K•, which corresponds to the ranking of the antioxidant and/or autooxidation potency of these three flavonoids [43].

The dietary flavonoid MYR is currently of interest because of its various pharmacological activities, such as antioxidant, anticancer, anti-inflammatory, neuroprotective and antibacterial effects. Interestingly, a recent study reported that MYR showed antiviral and prophylactic effects against COVID-19 [44]. However, our previous study showed anti- and pro-oxidant activities of a flavonoid procyanidin B2 [45], indicating that this flavonoid is a 'double-edged sword'. Furthermore, we demonstrated previously that several flavonoids exert pro-oxidant properties [46,47]. This study demonstrated that MYR causes site-specific DNA damage via ROS generation by redox interactions with copper ions. Previous studies have shown that MYR can generate ROS in the presence of transition metal ions with or without molecular DNA [9–12]. ROS is a significant player in oxidative DNA damage in vivo [48,49]. Thus, in the future, evaluating the safety of MYR in vivo is desirable when considering potential biomedical applications of MYR.

Declaration of Competing Interest

The authors declare that they have no known competing financial interests or personal relationships that could have appeared to influence the work reported in this paper.

Data Availability

Data will be made available on request.

Acknowledgments

This work was supported by JSPS KAKENHI Grant Numbers, 18K19673, 19H03885, 23H03148.

Appendix A. Supporting information

Supplementary data associated with this article can be found in the online version at doi:10.1016/j.mrgentox.2023.503694.

References

[1] N. Afroze, S. Pramodh, A. Hussain, M. Waleed, K. Vakharia, A review on myricetin as a potential therapeutic candidate for cancer prevention, 3 Biotech 10 (2020) 211.
[2] F. Panza, M. Lozupone, G. Logroscino, B.P. Imbimbo, A critical appraisal of amyloid-β-targeting therapies for Alzheimer disease, Nat. Rev. Neurol. 15 (2019) 73–88.
[3] K. Ono, L. Li, Y. Takamura, Y. Yoshiike, L. Zhu, F. Han, X. Mao, T. Ikeda, J. Takasaki, H. Nishijo, A. Takashima, D.B. Teplow, M.G. Zagorski, M. Yamada, Phenolic compounds prevent amyloid beta-protein oligomerization and synaptic dysfunction by site-specific binding, J. Biol. Chem. 287 (2012) 14631–14643.
[4] T. Hamaguchi, K. Ono, A. Murase, M. Yamada, Phenolic compounds prevent Alzheimer's pathology through different effects on the amyloid-beta aggregation pathway, Am. J. Pathol. 175 (2009) 2557–2565.
[5] M.E. Kim, T.K. Ha, J.H. Yoon, J.S. Lee, Myricetin induces cell death of human colon cancer cells via BAX/BCL2-dependent pathway, Anticancer Res 34 (2014) 701–706.
[6] N.J. Kang, S.K. Jung, K.W. Lee, H.J. Lee, Myricetin is a potent chemopreventive phytochemical in skin carcinogenesis, Ann. N. Y Acad. Sci. 1229 (2011) 124–132.
[7] M.S. Geybels, B.A. Verhage, I.C. Arts, F.J. van Schooten, R.A. Goldbohm, P.A. van den Brandt, Dietary flavonoid intake, black tea consumption, and risk of overall and advanced stage prostate cancer, Am. J. Epidemiol. 177 (2013) 1388–1398.
[8] C.A. Hobbs, C. Swartz, R. Maronpot, J. Davis, L. Recio, M. Koyanagi, S.M. Hayashi, Genotoxicity evaluation of the flavonoid, myricitrin, and its aglycone, myricetin, Food Chem. Toxicol. 83 (2015) 283–292.
[9] S.C. Sahu, G.C. Gray, Interactions of flavonoids, trace metals, and oxygen: nuclear DNA damage and lipid peroxidation induced by myricetin, Cancer Lett. 70 (1993) 73–79.
[10] M. Yoshino, M. Haneda, M. Naruse, K. Murakami, Prooxidant activity of flavonoids: copper-dependent strand breaks and the formation of 8-hydroxy-2′-deoxyguanosine in DNA, Mol. Genet. Metab. 68 (1999) 468–472.
[11] H. Arif, A. Sohail, M. Farhan, A.A. Rehman, A. Ahmad, S.M. Hadi, Flavonoids-induced redox cycling of copper ions leads to generation of reactive oxygen species: A potential role in cancer chemoprevention, Int. J. Biol. Macromol. 106 (2018) 569–578.
[12] M. Said Ahmad, F. Fazal, A. Rahman, S.M. Hadi, J.H. Parish, Activities of flavonoids for the cleavage of DNA in the presence of Cu(II): correlation with generation of active oxygen species, Carcinogenesis 13 (1992) 605–608.
[13] M. Serrano, G.J. Hannon, D. Beach, A new regulatory motif in cell-cycle control causing specific inhibition of cyclin D/CDK4, Nature 366 (1993) 704–707.
[14] D.J. Capon, E.Y. Chen, A.D. Levinson, P.H. Seeburg, D.V. Goeddel, Complete nucleotide sequences of the T24 human bladder carcinoma oncogene and its normal homologue, Nature 302 (1983) 33–37.
[15] S. Oikawa, K. Murakami, S. Kawanishi, Oxidative damage to cellular and isolated DNA by homocysteine: implications for carcinogenesis, Oncogene 22 (2003) 3530–3538.
[16] S. Oikawa, K. Yamada, N. Yamashita, S. Tada-Oikawa, S. Kawanishi, N-acetylcysteine, a cancer chemopreventive agent, causes oxidative damage to cellular and isolated DNA, Carcinogenesis 20 (1999) 1485–1490.
[17] S. Kawanishi, K. Yamamoto, Mechanism of site-specific DNA damage induced by methylhydrazines in the presence of copper(II) or manganese(III), Biochemistry 30 (1991) 3069–3075.
[18] K. Yamamoto, S. Kawanishi, Site-specific DNA damage induced by hydrazine in the presence of manganese and copper ions. The role of hydroxyl radical and hydrogen atom, J. Biol. Chem. 266 (1991) 1509–1515.

[19] A.M. Maxam, W. Gilbert, Sequencing end-labeled DNA with base-specific chemical cleavages, Methods Enzym. 65 (1980) 499–560.
[20] K. Kawai, H. Kasai, Y.S. Li, Y. Kawasaki, S. Watanabe, M. Ohta, T. Honda, H. Yamato, Measurement of 8-hydroxyguanine as an oxidative stress biomarker in saliva by HPLC-ECD, Genes Environ. 40 (2018) 5.
[21] Y. Mori, S. Kato, Y. Fujisawa, S. Ohnishi, Y. Hiraku, S. Kawanishi, M. Murata, S. Oikawa, Mechanisms of DNA damage induced by morin, an inhibitor of amyloid β-peptide aggregation, Free Radic. Res. 53 (2019) 115–123.
[22] H. Kobayashi, Y. Mori, R. Iwasa, Y. Hirao, S. Kato, S. Kawanishi, M. Murata, S. Oikawa, Copper-mediated DNA damage caused by purpurin, a natural anthraquinone, Genes Environ. 44 (2022) 15.
[23] Y.-S. Li, M.-F. Song, H. Kasai, K. Kawai, Generation and threshold level of 8-OHdG as oxidative DNA damage elicited by low dose ionizing radiation, Genes Environ. 35 (2013) 88–92.
[24] S. Oikawa, H. Kobayashi, S. Tada-Oikawa, Y. Isono, S. Kawanishi, Damage to cellular and isolated DNA induced by a metabolite of aspirin, Mutat. Res. 661 (2009) 93–100.
[25] K. Satou, M. Hori, K. Kawai, H. Kasai, H. Harashima, H. Kamiya, Involvement of specialized DNA polymerases in mutagenesis by 8-hydroxy-dGTP in human cells, DNA Repair 8 (2009) 637–642.
[26] I. Kasugai, M. Yamada, High production of catalase in hydrogen peroxide-resistant human leukemia HL-60 cell lines, Leuk. Res. 16 (1992) 173–179.
[27] W.A. Pryor, R.H. Tang, Ethylene formation from methional, Biochem. Biophys. Res. Commun. 81 (1978) 498–503.
[28] J.H. Northrop, The kinetics of the decomposition of peroxide by catalase, J. Gen. Physiol. 7 (1925) 373–387.
[29] V.A. Rapisarda, S.I. Volentini, R.N. Farías, E.M. Massa, Quenching of bathocuproine disulfonate fluorescence by Cu(I) as a basis for copper quantification, Anal. Biochem. 307 (2002) 105–109.
[30] S. Ohnishi, Y. Hiraku, K. Hasegawa, K. Hirakawa, S. Oikawa, M. Murata, S. Kawanishi, Mechanism of oxidative DNA damage induced by metabolites of carcinogenic naphthalene, Mutat. Res. 827 (2018) 42–49.
[31] Y. Mori, H. Kobayashi, Y. Fujita, M. Yatagawa, S. Kato, S. Kawanishi, M. Murata, S. Oikawa, Mechanism of reactive oxygen species generation and oxidative DNA damage induced by acrylohydroxamic acid, a putative metabolite of acrylamide, Mutat. Res. 873 (2022), 503420.
[32] M.H. Chung, H. Kiyosawa, E. Ohtsuka, S. Nishimura, H. Kasai, DNA strand cleavage at 8-hydroxyguanine residues by hot piperidine treatment, Biochem. Biophys. Res. Commun. 188 (1992) 1–7.
[33] H. Kasai, M.H. Chung, D.S. Jones, H. Inoue, H. Ishikawa, H. Kamiya, E. Ohtsuka, S. Nishimura, 8-Hydroxyguanine, a DNA adduct formed by oxygen radicals: its implication on oxygen radical-involved mutagenesis/carcinogenesis, J. Toxicol. Sci. 16 (Suppl 1) (1991) 95–105.
[34] S. Oikawa, K. Murakami, S. Kawanishi, Oxidative damage to cellular and isolated DNA by homocysteine: implications for carcinogenesis, Oncogene 22 (2003) 3530–3538.
[35] S. Shibutani, M. Takeshita, A.P. Grollman, Insertion of specific bases during DNA synthesis past the oxidation-damaged base 8-oxodG, Nature 349 (1991) 431–434.
[36] R.A. Floyd, The role of 8-hydroxyguanine in carcinogenesis, Carcinogenesis 11 (1990) 1447–1450.
[37] N. Fujii, S. Yano, K. Takeshita, Selective enhancing effect of metal ions on mutagenicity, Genes Environ. 38 (2016) 21.
[38] M.C. Linder, The relationship of copper to DNA damage and damage prevention in humans, Mutat. Res 733 (2012) 83–91.
[39] M. Fatfat, R.A. Merhi, O. Rahal, D.A. Stoyanovsky, A. Zaki, H. Haidar, V.E. Kagan, H. Gali-Muhtasib, K. Machaca, Copper chelation selectively kills colon cancer cells through redox cycling and generation of reactive oxygen species, BMC Cancer 14 (2014) 527.
[40] D. Denoyer, S.A. Clatworthy, S. Masaldan, P.M. Meggyesy, M.A. Cater, Heterogeneous copper concentrations in cancerous human prostate tissues, Prostate 75 (2015) 1510–1517.
[41] N. Yamashita, H. Tanemura, S. Kawanishi, Mechanism of oxidative DNA damage induced by quercetin in the presence of Cu(II), Mutat. Res. 425 (1999) 107–115.
[42] Z. Li, M. Moalin, M. Zhang, L. Vervoort, A. Mommers, G. Haenen, Delocalization of the unpaired electron in the quercetin radical: comparison of experimental ESR data with DFT calculations, Int. J. Mol. Sci. 21 (2020).
[43] J. Krych-Madej, K. Stawowska, L. Gebicka, Oxidation of flavonoids by hypochlorous acid: reaction kinetics and antioxidant activity studies, Free Radic. Res. 50 (2016) 898–908.
[44] P.K. Agrawal, C. Agrawal, G. Blunden, Antiviral and possible prophylactic significance of myricetin for COVID-19, Nat. Prod. Comm. 18 (2023), 1934578×231166283.
[45] K. Sakano, M. Mizutani, M. Murata, S. Oikawa, Y. Hiraku, S. Kawanishi, Procyanidin B2 has anti- and pro-oxidant effects on metal-mediated DNA damage, Free Radic. Biol. Med. 39 (2005) 1041–1049.
[46] H. Kobayashi, M. Murata, S. Kawanishi, S. Oikawa, Polyphenols with anti-amyloid β aggregation show potential risk of toxicity via pro-oxidant properties, Int. J. Mol. Sci. 21 (2020).
[47] S. Kawanishi, S. Oikawa, M. Murata, Evaluation for safety of antioxidant chemopreventive agents, Antioxid. Redox Signal 7 (2005) 1728–1739.
[48] B. Halliwell, A. Adhikary, M. Dingfelder, M. Dizdaroglu, Hydroxyl radical is a significant player in oxidative DNA damage in vivo, Chem. Soc. Rev. 50 (2021) 8355–8360.
[49] H. Nakamura, K. Takada, Reactive oxygen species in cancer: current findings and future directions, Cancer Sci. 112 (2021) 3945–3952.

Figure S1

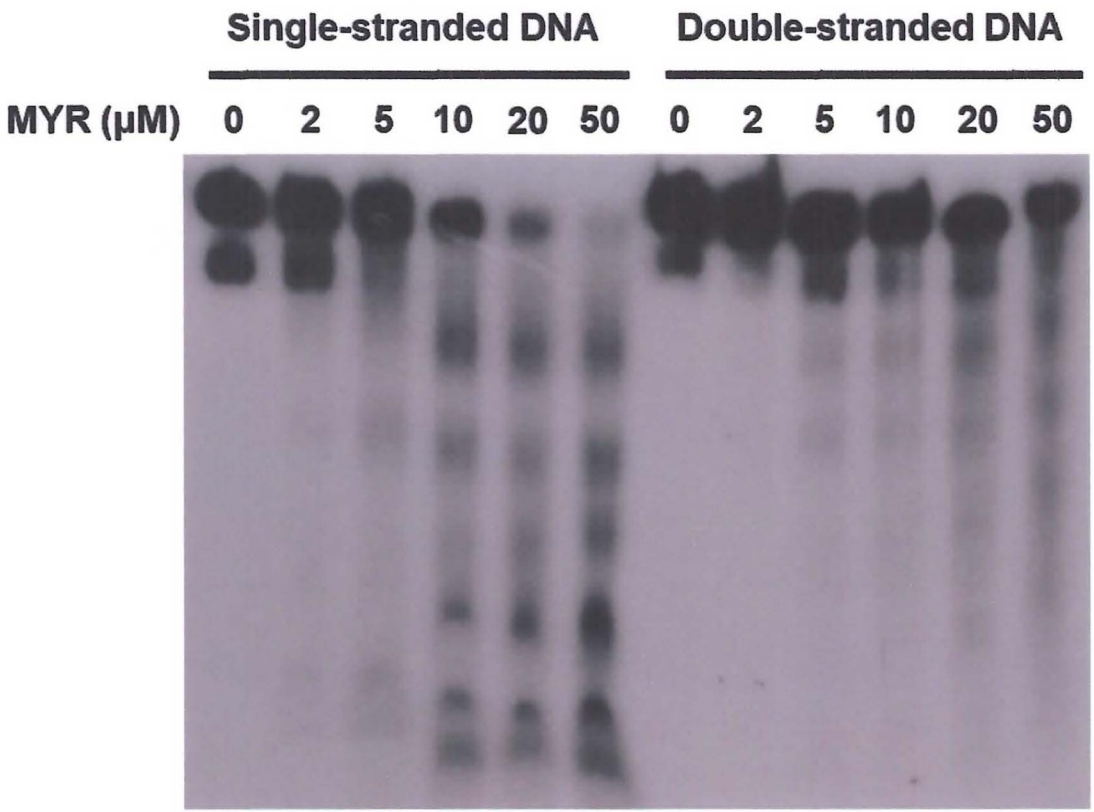

Fig. S1. Autoradiogram of ^{32}P-5′-end-labeled DNA fragments incubated with MYR+Cu. Reaction mixtures contained the ^{32}P-5′-end-labeled 147 bp fragment, 20 μM/base calf thymus DNA, the indicated concentrations of MYR and 20 μM $CuCl_2$ in 10 mM sodium phosphate buffer (pH 7.8) containing 5 μM DTPA. Denatured single-stranded DNA fragments were prepared by heating at 90°C for 5 min followed by quick chilling before the addition of MYR. After incubation at 37°C for 0.5 h under light shielding, the DNA fragments were treated with piperidine and electrophoresed on a polyacrylamide gel.

Figure S2

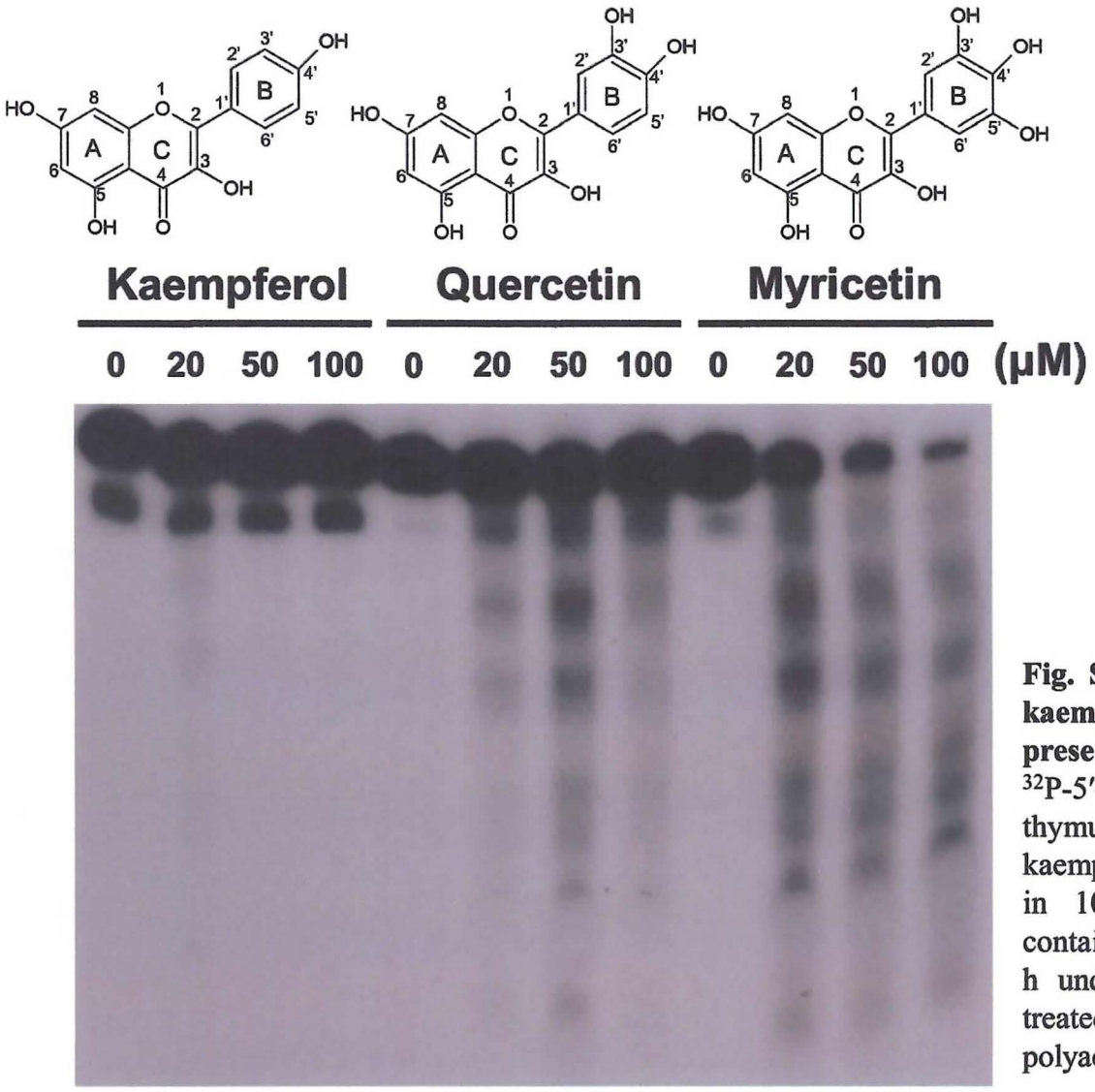

Fig. S2. Comparison of DNA damage induced by kaempferol, quercetin and myricetin in the presence of Cu(II). Reaction mixtures contained the ^{32}P-5′-end-labeled 147 bp fragment, 20 μM/base calf thymus DNA, the indicated concentrations of kaempferol, quercetin or myricetin and 20 μM $CuCl_2$ in 10 mM sodium phosphate buffer (pH 7.8) containing 5 μM DTPA. After incubation at 37°C for 1 h under light shielding, the DNA fragments were treated with piperidine and electrophoresed on a polyacrylamide gel.